Radiative
Atmospheric
Divergence using
ARM Mobile Facility
GERB data and
AMMA STations

radagast.nerc-essc.ac.uk

Identifying and Modelling Clear-sky Fluxes using the AMF in Niamey and GERB/SEVIRI on Meteosat 8

Nazim Ali Bharmal, Anthony Slingo, Gary Robinson

Environmental Systems Science Centre, University of Reading

nab@mail.nerc-essc.ac.uk

NATURAL ENVIRONMENT RESEARCH COUNCIL
ENVIRONMENTAL SYSTEMS SCIENCE CENTRE

Imperial College London

1. Introduction

Aerial view of AMF deployment, Niamey airport. Image © TerraMetrics

RADAGAST employs measurements of the Earth's radiation, *via* the ARM AMF deployment in Niger and the GERB instrument on the Meteosat 8 geostationary satellite. A program of modelling using several radiation codes, including Edwards-Slingo, has been undertaken. The initial results and the consequences for modelling are presented here.

The approach described here is to model the 'clear-sky' profiles (cloud- and aerosol-free), with the aim of using the results for inferring forcings from the two major sources of radiative perturbation in Niger: clouds and aerosols.

The results are split into understanding and identifying the clear-sky flux at the top-of-atmosphere, and progress in modelling long-wave fluxes and radiances at the ground.

3. Modelling long-wave fluxes & radiances

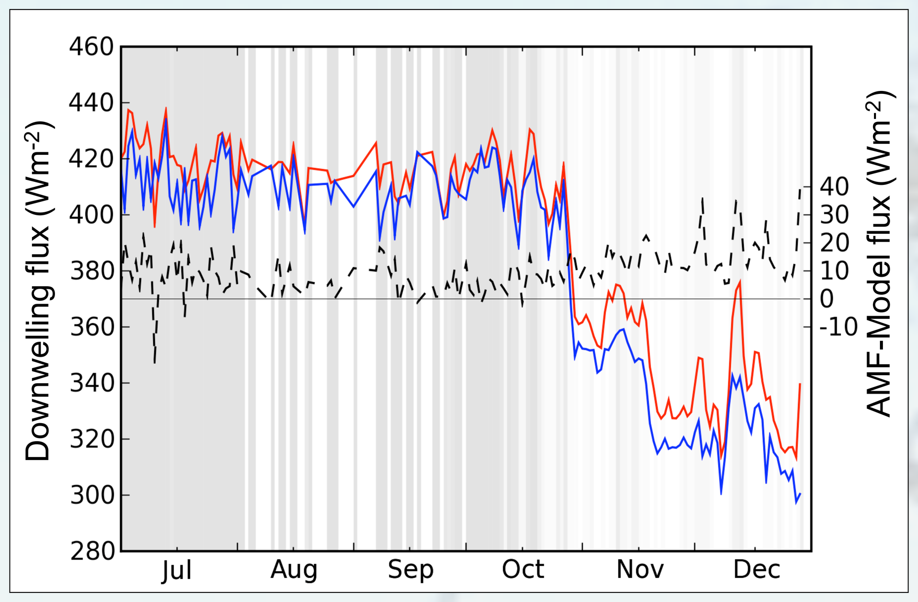

Figure 5: Daily-averaged down-welling LW flux, from AMF measurements (red) and modelled results (blue). The difference is shown by the dashed line, cloud cover forms the background.

The Edwards-Slingo radiative transfer code was used with atmospheric profiles created using several ARM instruments (including rawinsondes). Figure 5 shows both the daily mean down-welling clear-sky LW flux from the model and the measurement from the AMF, Niamey. There is a noticeable difference in the latter part of the year - a period with low column water vapour.

There is significant variation in aerosol loading during November; these changes do not, however, significantly alter the flux differences. Thus variable aerosol loading is discounted as an important factor.

An alternative measurement of LW radiation is via the AERI interferometer. Figure 6 shows a calculation from one profile in late November. It also shows the model under-representing the measured radiation. A comparison of fluxes calculated using Edwards-Slingo RT code (by the lead author) and independent calculations using LBLRTM (courtesy Eli Mlawer) is shown in figure 7. There are disagreements of ~3 Wm^{-2}, but the overall trend lies well to the right of the 1:1 line. The cause of all these disagreements has not yet been established.

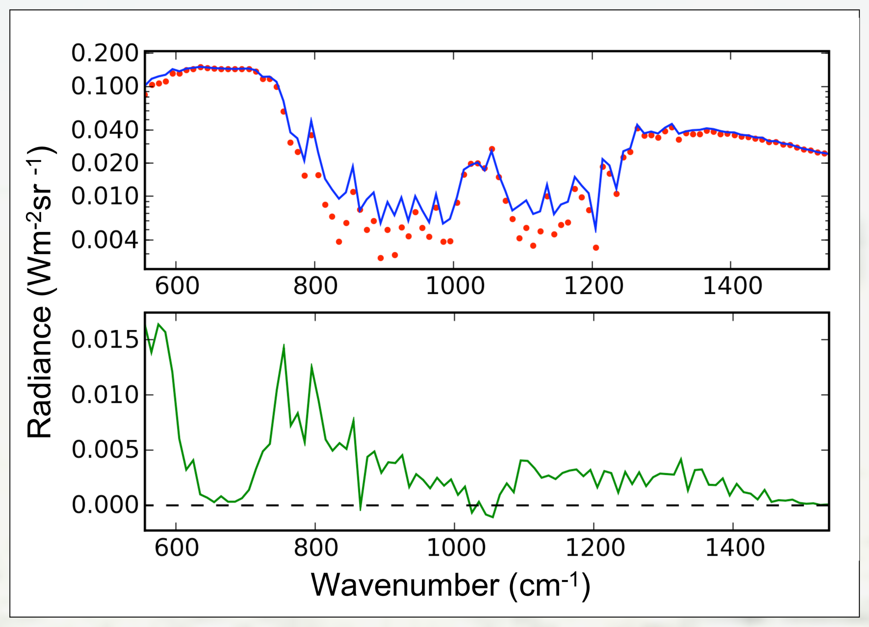

Figure 6: Down-welling LW radiances for one profile (2006/11/25 at 23h00). The AERI measurements (blue) are binned into the 10cm^{-1} bins used by the Edwards-Slingo RT code results (red). The green line shows the measurement-model difference. Column water vapour is ~0.7cm.

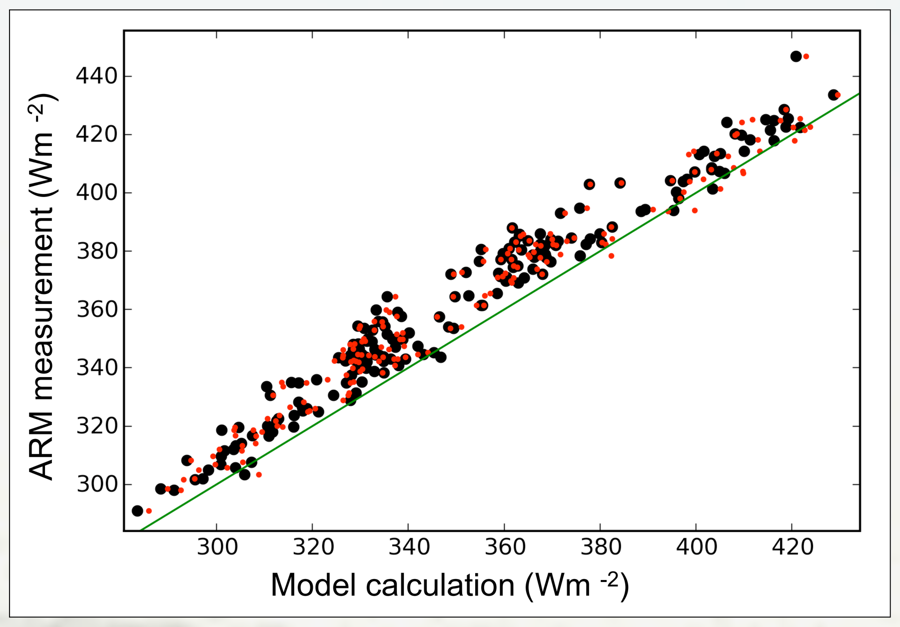

Figure 7: Scatter plot of down-welling LW fluxes. Each point corresponds to a 'sonde launch where there is no cloud cover: calculations were made for each resulting profile using both LBLRTM (black) and Edwards-Slingo (red). The time period covered is between July & December 2006.

2. Identifying and comparing clear-sky fluxes

The flux modelling undertaken assumes a plane-parallel atmosphere. However, the measurements from the AMF are those of a point source on the ground, whereas satellite measurements from GERB or SEVIRI instruments cover a large, heterogeneous area.

The difficulty this can cause is demonstrated in figure 1, which shows the top-of-atmosphere short-wave flux from the product pixel covering the AMF: *via* the GERB ARG product (50km x 50km pixel); and *via* the GERB/SEVIRI HR product (10km x 10km pixel).

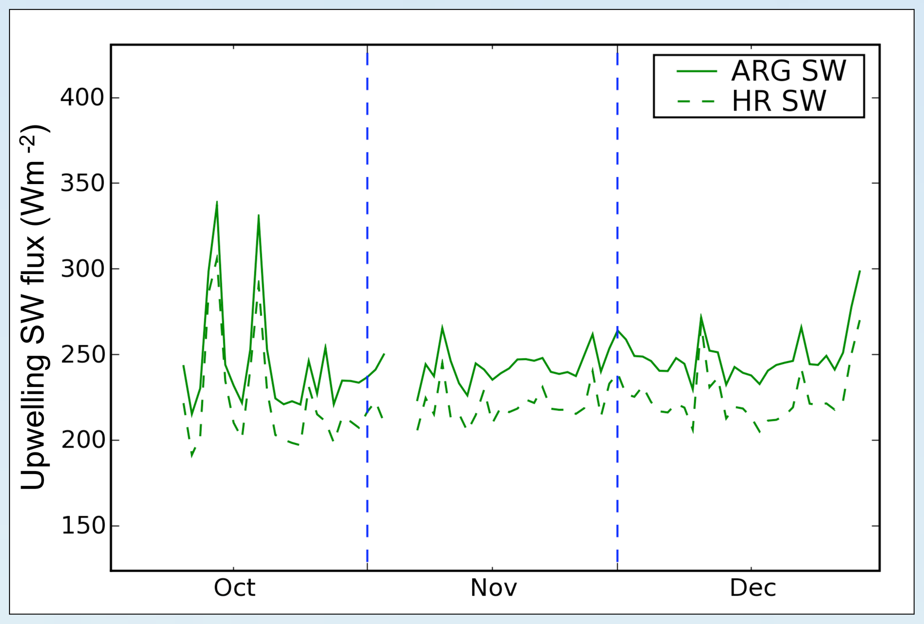

Figure 1: TOA SW fluxes via two products from satellite measurements: ARG and HR.

The difference between the two fluxes is sizeable (~20 Wm^{-2}), and is explained by figure 2. This shows visible SEVIRI radiances (3km x 3km pixels) over the ARG pixel-area.

The HR pixel, however, covers a much smaller area and is thus associated with lower albedo. Compared to the ARG area, the ratio of radiances in the ARG pixel to those from the HR pixel is 1.09. The corresponding ratio of fluxes from figure 1 is 1.10±0.02. For more discussion on heterogeneity, please see the Settle *et al.* poster.

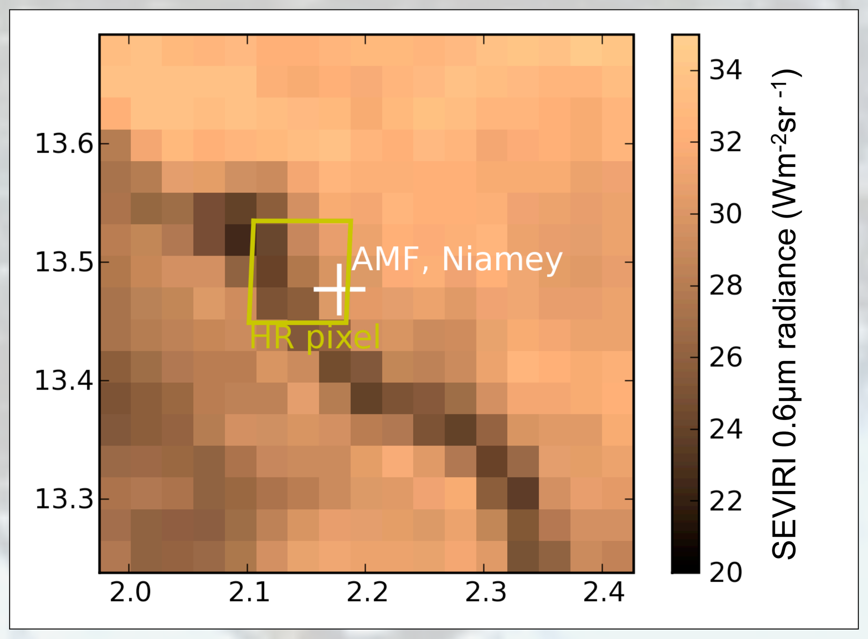

Figure 2: 0.6μm SEVIRI radiances. Mean of all times during November 2006 without cloud-cover. The dark band is the Niger river.

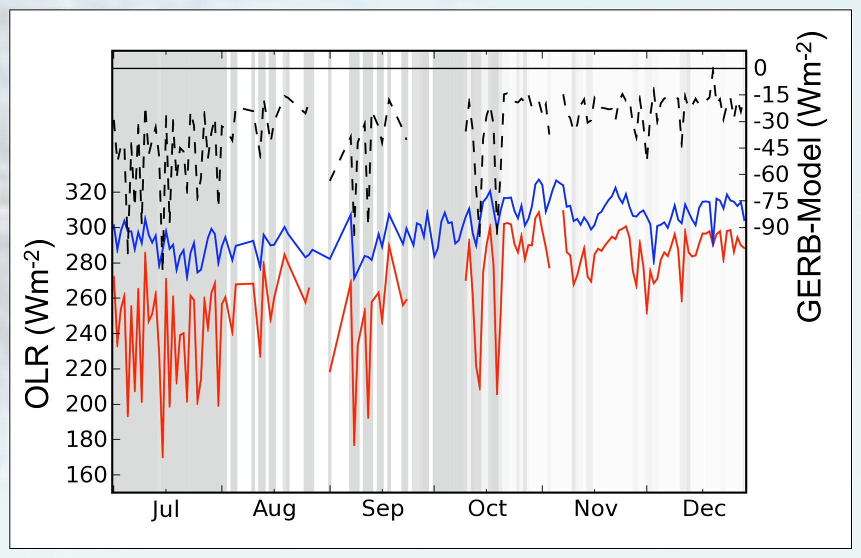

Figure 3: Daily average outgoing LW flux (OLR) from the GERB ARG product (red) and the modelling (blue). The difference is the dashed line, and cloud cover forms the background.

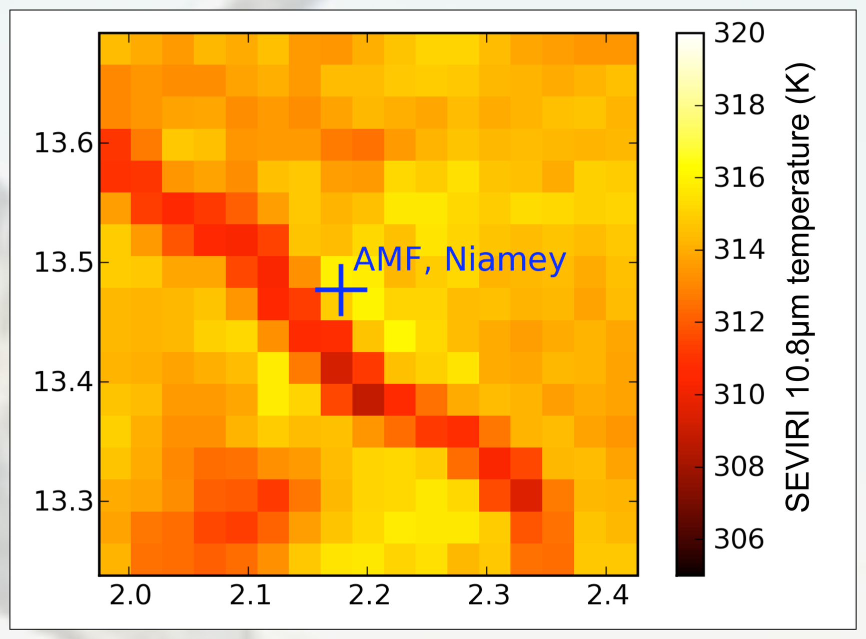

Figure 4: 10.8μm SEVIRI brightness temperatures. Mean of all 12h00 during November 2006 without cloud-cover.

A corresponding result can be seen in the top-of-atmosphere long-wave flux. Figure 3 shows the modelled OLR and that measured by the ARG product. The difference is postulated to be because the AMF ground measurements are not representative of the area within the ARG pixel. Figure 4 shows the SEVIRI 10.8μm-derived skin temperatures: over the region, the temperature variations can account for an upwelling flux variation of 70 Wm^{-2}. At the AMF, Niamey airport site itself, the November-averaged skin temperature is ~319K.

Acknowledgements: this poster shows work-in-progress, which has been considerably aided thanks to the ARM archive (AMF data); Royal Met. Inst. of Belgium, Imperial College, Rutherford Appleton Laboratories, EUMETSAT (GERB/SEVIRI data), ECMWF, UK Met Office, colleagues at PNNL, and Eli Mlawer (LBLRTM calculations / AER Inc.).